Quantum dynamics of cold atomic gas with SU(1,1) symmetry

Jing Zhang, Xiaoyi Yang, Chenwei Lv, Shengli Ma, and Ren Zhang

Quantum Dynamics of Cold Atomic Gas with $SU(1,1)$ Symmetry

Jing Zhang,[1,2] Xiaoyi Yang,[1,2] Chenwei Lv,[3,*] Shengli Ma,[1,2,†] and Ren Zhang[1,2,‡]

[1]*School of Physics, Xi'an Jiaotong University, Xi'an 710049, Shaanxi, China*
[2]*Shaanxi Province Key Laboratory of Quantum Information and Quantum Optoelectronic Devices,*
Xi'an Jiaotong University, Xi'an 710049, Shaanxi, China
[3]*Department of Physics and Astronomy, Purdue University, West Lafayette, IN, 47907, USA*
(Dated: July 11, 2022)

Motivated by recent advances in quantum dynamics, we investigate the dynamics of the system with $SU(1,1)$ symmetry. Instead of performing the time-ordered integral for the evolution operator of the time-dependent Hamiltonian, we show that the time evolution operator can be expressed as a $SU(1,1)$ group element. Since the $SU(1,1)$ group describes the "rotation" on a hyperbolic surface, the dynamics can be visualized on a Poincaré disk, a stereographic projection of the upper hyperboloid. As an example, we present the trajectory of the revival of Bose-Einstein condensation and that of the scale-invariant Fermi gas on the Poincaré disk. Further considering quantum gases in an oscillating lattice, we also study the dynamics of the system with time-dependent single-particle dispersion.

I. INTRODUCTION

The study of quantum dynamics has attracted extensive recent interests in cold atom physics. One of the prominent advantages of cold atom physics is the flexibility in quantum manipulation. Both the single-particle Hamiltonian and the pairwise interaction can be precisely controlled by external fields [1, 2]. Using the optical lattice and Feshbach resonance, one can tune the single-particle dispersion and the interaction strength, respectively. As a result, quantum dynamics in cold atomic gases can be studied in a controllable manner.

Recently, an experimental group from Chicago discovered a series of intriguing dynamics in Bose gases by implementing an oscillating interaction, such as the Bose fireworks [3] and the revival of Bose-Einstein condensation (BEC) [4, 5]. In a quasi-two-dimensional potential, the spatial configuration of a Bose gas can be manipulated. For instance, the box potential [6, 7], circle potential [8], and triangle potential [9] have been realized. The experimental group from ENS observed that BEC in the circle and triangle potential revives after an appropriate time [9], which is quite counterintuitive as the initial state of a many-body system usually does not revive. For Fermi gas in a harmonic trapping potential with unitary or without interaction, the system size shows a discrete scaling law when the trapping frequency varies in a proper way. This phenomenon is named as "Efimovian expansion" [10–12]. These experiments are quite distinct in the aspects of statistics, dimensionality, and extra confinement. However, they share the common feature that the dynamics can be captured by the $SU(1,1)$ group.

It is instructive to compare the $SU(1,1)$ and $SU(2)$ group [13]. Similar to $SU(2)$, the $SU(1,1)$ group is generated by three operators $\hat{K}_0$, $\hat{K}_1$ and $\hat{K}_2$ which satisfy the

* lvc@purdue.edu
† msl1987@xjtu.edu.cn
‡ renzhang@xjtu.edu.cn

commutation relation $[\hat{K}_1, \hat{K}_2] = -i\hat{K}_0, [\hat{K}_0, \hat{K}_1] = i\hat{K}_2$ and $[\hat{K}_2, \hat{K}_0] = i\hat{K}_1$ [14, 15]. It is known that $SU(2)$ group describes the rotation on a Bloch sphere, while the $SU(1,1)$ group describes the "rotation" on a hyperbolic surface [16, 17]. Using the commutation relation, one can show that $\hat{K}_0$ generates the usual rotation around a particular axis, say, the z-axis. $\hat{K}_1$ and $\hat{K}_2$ generate the pseudo-rotation (or boost) along the y- and x-axis, respectively. To be specific,

$$e^{-i\theta\hat{K}_0}\hat{K}_{1(2)}e^{i\theta\hat{K}_0} = \hat{K}_{1(2)}\cos\theta + (-)\hat{K}_{2(1)}\sin\theta; \quad (1)$$

$$e^{-i\theta\hat{K}_1}\hat{K}_{2(0)}e^{i\theta\hat{K}_1} = \hat{K}_{2(0)}\cosh\theta - \hat{K}_{0(2)}\sinh\theta; \quad (2)$$

$$e^{-i\theta\hat{K}_2}\hat{K}_{0(1)}e^{i\theta\hat{K}_2} = \hat{K}_{0(1)}\cosh\theta + \hat{K}_{1(0)}\sinh\theta, \quad (3)$$

where θ is the (pseudo-)rotation angle [14]. With the aid of this geometric picture, the quantum dynamics can be visualized on the Poincaré disk, a stereographic projection of upper hyperboloid. It provides a straightforward intuition of the quantum dynamics of a many-body system. The studies on the dynamics of BEC and the breathing mode in quantum gases are underpinned by the $SU(1,1)$ group [18–28], and it can be visualized for arbitrary initial state [29, 30]. As such, it is natural to generalize the geometric visualization to more systems, the dynamics of which are governed by the $SU(1,1)$ group.

Another benefit of implementing the $SU(1,1)$ group is the simplification of the calculation for the quantum dynamics, even when the Hamiltonian is time-dependent [31]. The conventional wisdom for evaluating the quantum evolution is to perform the time-ordered integral, which is numerically time-consuming. The analytical treatment is only available when the interaction is perturbative. Nevertheless, when the Hamiltonian is expressed as the linear combination of the $SU(1,1)$ generators, the evolution operator becomes a $SU(1,1)$ group element. As such, the evolution can be obtained analytically, which enables us to investigate the quantum dynamics in a generic manner.

As of now, the dynamics dominated by the manipula-

tion of the pairwise interaction and the external potential have been intensively studied. A natural question arises. What happens if the single-particle dispersion is time-dependent? This can be achieved by considering cold atoms in a periodic driven optical lattice with oscillating depth. As a result, the bandwidth of a tight-binding model becomes time-dependent. If low-energy physics is concerned, a time-dependent effective mass will dominate the dynamics [32].

The arrangement of this manuscript is as follows. In Section II, we present the general formalism for the quantum dynamics with $SU(1,1)$ symmetry. In Section III, the geometric visualization for BEC and scale-invariant Fermi gases are shown. Then, the dynamics of quantum gases in an oscillating optical lattice is studied in Section IV. At last, we summarize our results in Section V.

II. GENERAL FORMULISM

In this manuscript, the Hamiltonian we are considering is of the following generic form

$$\hat{H}(t) = \alpha(t)\hat{K}_0 + \beta(t)\hat{K}_1, \tag{4}$$

where $\alpha(t)$ and $\beta(t)$ are time-dependent. The absence of $\hat{K}_2$ does not affect the generality, since an extra term $\gamma(t)\hat{K}_2$ could be removed by $e^{-i\arctan(\gamma(t)/\beta(t))\hat{K}_0}$. For different systems, the definition of $\hat{K}_i$ varies. To study the dynamics, the most direct approach is to evaluate the evolution operator $\hat{U}(t,0) = \hat{\mathcal{T}}\exp\left(-i\int_0^t \hat{H}(\tau)d\tau\right)$, where $\hat{\mathcal{T}}$ denotes the time-ordering operator. However, this method becomes formidable in the many-body system, due to the exponentially increase of the Hilbert space dimension. Since the commutation relation is closed, the evolution operator can be written as [31]

$$\hat{U}(t,0) = e^{\zeta_+(t)\hat{K}_+}e^{\hat{K}_0 \ln \eta(t)}e^{\zeta_-(t)\hat{K}_-}, \tag{5}$$

where $\zeta_\pm(t)$ and $\eta(t)$ are functions of $\alpha(t), \beta(t)$, and $\hat{K}_\pm \equiv \hat{K}_1 \pm i\hat{K}_2$ are the ladder operators. To be specific, we define $|k,j\rangle$ as the common eigenstates of $\hat{K}_0$ and the Casimir operator $\hat{C} = \hat{K}_0^2 - \hat{K}_1^2 - \hat{K}_2^2$, that is, $\hat{K}_0|k,j\rangle = j|k,j\rangle$ and $\hat{C}|k,j\rangle = k(k-1)|k,j\rangle$. It can be proved that $\hat{K}_\pm|k,j\rangle \propto |k,j\pm 1\rangle$. The requirement that $\langle k,j|\hat{K}_\mp\hat{K}_\pm|k,j\rangle \geq 0$, i.e., $j(j\pm 1) - k(k-1) \geq 0$ indicates that j is bounded from below with $j_{\min} = k$. The Hilbert space spanned by $\{|k,k\rangle, \hat{K}_+|k,k\rangle, \hat{K}_+^2|k,k\rangle, ...\}$ constitutes a representation of the $SU(1,1)$ group. In this manuscript, we focus on this representation and denote the ground state of $\hat{K}_0$ as $|k,k\rangle$.

To determine the coefficients $\zeta_\pm(t)$ and $\eta(t)$, we could solve the differential equation of the evolution operator $i\partial_t\hat{U}(t,0) = \hat{H}(t)\hat{U}(t,0)$, which can be recast as

$$\frac{\partial_t\hat{U}(t,0)}{\hat{U}(t,0)} = -i\alpha(t)\hat{K}_0 - \frac{i}{2}\beta(t)(\hat{K}_+ + \hat{K}_-). \tag{6}$$

This approach is straightforward but formidable in the many-body system. It is straightforward to prove the following equation from Eq. (5),

$$\frac{\partial_t\hat{U}(t,0)}{\hat{U}(t,0)} = \frac{1}{\eta(t)}\left[\frac{\partial\eta(t)}{\partial t} - 2\zeta_+(t)\frac{\partial\zeta_-(t)}{\partial t}\right]\hat{K}_0$$
$$+ \left[\frac{\partial\zeta_+(t)}{\partial t} - \frac{\zeta_+(t)}{\eta(t)}\frac{\partial\eta(t)}{\partial t} + \frac{\zeta_+(t)^2}{\eta(t)}\frac{\partial\zeta_-(t)}{\partial t}\right]\hat{K}_+$$
$$+ \frac{1}{\eta(t)}\frac{\partial\zeta_-(t)}{\partial t}\hat{K}_-. \tag{7}$$

For the detailed derivation, please refer to Appendix A. Comparing the right hand side of Eq. (6) and Eq. (7), we immediately obtain the following set of equations,

$$-i\alpha(t) = \frac{1}{\eta(t)}\left[\frac{\partial\eta(t)}{\partial t} - 2\zeta_+(t)\frac{\partial\zeta_-(t)}{\partial t}\right]; \tag{8}$$

$$-\frac{i}{2}\beta(t) = \frac{\partial\zeta_+(t)}{\partial t} - \frac{\zeta_+(t)}{\eta(t)}\frac{\partial\eta(t)}{\partial t} + \frac{\zeta_+(t)^2}{\eta(t)}\frac{\partial\zeta_-(t)}{\partial t}; \tag{9}$$

$$-\frac{i}{2}\beta(t) = \frac{1}{\eta(t)}\frac{\partial\zeta_-(t)}{\partial t}. \tag{10}$$

This set of equations plays a central role in the study of quantum dynamics. In the following sections, we will apply these results to different cases. Solving this set of algebraic equations under the initial conditions $\zeta_\pm(0) = 0, \eta(0) = 1$ and implementing the evolution operator defined in Eq. (5) to the initial state, the dynamics of a system can be obtained. The initial time is set as $t_0 = 0$. We would like to point out that our approach is valid for any system with the Hamiltonian of the form in Eq. (4), and is independent of the dimensionality, statistics, and interaction strength.

In case that the initial state $|\psi_i\rangle = |k,k\rangle$ is the ground state of $\hat{K}_0$, $\hat{K}_-|\psi_i\rangle = 0$, the evolution operator can be further simplified as $\hat{U}(t,0) = \eta(t)^k e^{\zeta_+(t)\hat{K}_+}$. The effect of the evolution operator then becomes the same as a displacement operator $\hat{D}(\xi(t)) = \exp\left(\xi(t)\hat{K}_+ - \xi^*(t)\hat{K}_-\right)$ with $\zeta_+(t) = \frac{\xi(t)}{|\xi(t)|}\tanh|\xi(t)|$. Then the coherent state of $SU(1,1)$ group [16]

$$|\zeta_+(t),k\rangle = \left(1 - |\zeta_+(t)|^2\right)^k\sum_{n=0}^\infty \frac{1}{n!}\zeta_+^n(t)\hat{K}_+^n|k,k\rangle, \tag{11}$$

can be represented by a point on the Poincaré disk [29, 30]. As a result, the evolution of a series of systems with $SU(1,1)$ symmetry can be visualized on the Poincaré disk. In the next section, we use two examples to demonstrate this visualization.

III. QUANTUM DYNAMICS OF BOSE-EINSTEIN CONDENSATION AND SCALE-INVARIANT FERMI GAS

In this section, we implement the approach described in Section II to the bosonic and fermionic system. The
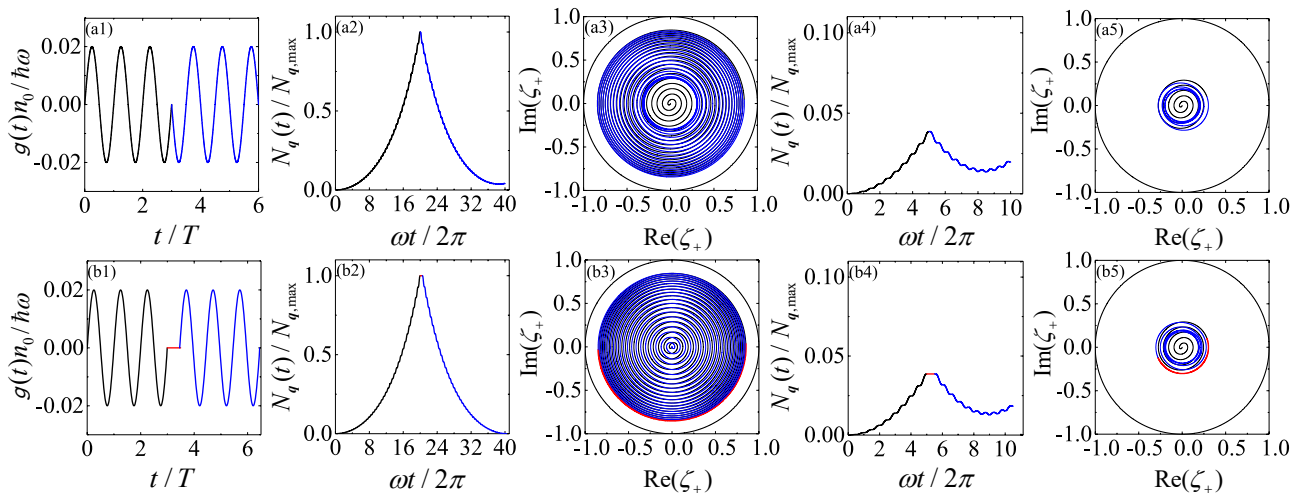
FIG. 1. Quantum dynamics of Bose-Einstein condensation under the oscillating s-wave scattering length. Oscillation schemes (I) and (II) are schematically shown in (a1) and (b1), respectively. (a2) and (b2): The respective resonant mode particle number as a function of time. Here we define the resonant mode as $\hbar^2 q_{\text{res}}^2/(2m) = \left(1/2 + 3\Delta^2/8\right)\hbar\omega$ with ω being the oscillating frequency. The non-monotonic profile indicates BEC revives, and the revival is perfect under the scheme (II). (a3) and (b3) are the visualizations of the quantum dynamics on Poincaré disk. For both schemes, the start point is the disk center. However, the ending point for scheme (I) is not the disk center and the ending point for scheme (II) is the disk center. The similar calculation for the non-resonant mode are shown in (a4,a5,b4,b5). Here, ζ_+ is dimensionless. In our calculation, the momentum of the non-resonant mode is $q = 0.99 q_{\text{res}}$, and the interaction strength is $g_0 n_0 = 0.02\hbar\omega$. $N_{\mathbf{q},\text{max}}$ is the maximum of $N_{\mathbf{q}}$ for the resonant mode.

revival of BEC and Efimovian expansion in the scale-invariant Fermi gas can be readily obtained, and evolutionary trajectories of the systems are shown on the Poincaré disk.

A. Revival of BEC

We start with the revival of BEC with the oscillating scattering length. In Ref. [4], the authors observed that the nonzero momentum particle number $N_{\mathbf{q}}$ exponentially increases when the s-wave scattering length a_s is sinusoidally varying. After some time, the phase of a_s suddenly changes by π, and $N_{\mathbf{q}}$ begins to decrease, that is, BEC begins to revive. The following theoretical work proposed a more efficient revival protocol by turning off the interaction for a while but keeping the phase invariant, which is named as the "Many-Body Echo" [26]. The $SU(1,1)$ echo, a counterpart of the spin echo [33, 34], has been proposed and explains the experimental observation [30]. The underlying reason for the revival of BEC is the $SU(1,1)$ symmetry of the Bogoliubov Hamiltonian that describes Bose gases with weak interaction. Specifically, the Bogoliubov Hamiltonian is written as $\hat{H}_{\text{Bog}} = \frac{g(t)N^2}{2V} + \sum_{\mathbf{q}\neq 0}\left(\hat{H}_{\text{Bog}}^{\mathbf{q}}(t) - \frac{\epsilon_{\mathbf{q}} + g(t)n_0}{2}\right)$ with

$$\hat{H}_{\text{Bog}}^{\mathbf{q}}(t) = \frac{(\epsilon_{\mathbf{q}} + g(t)n_0)}{2}\left(\hat{a}_{\mathbf{q}}^{\dagger}\hat{a}_{\mathbf{q}} + \hat{a}_{-\mathbf{q}}\hat{a}_{-\mathbf{q}}^{\dagger}\right)$$
$$+ \frac{g(t)n_0}{2}\left(\hat{a}_{\mathbf{q}}^{\dagger}\hat{a}_{-\mathbf{q}}^{\dagger} + \hat{a}_{\mathbf{q}}\hat{a}_{-\mathbf{q}}\right), \quad (12)$$

where $\hat{a}_{\mathbf{q}}^{\dagger}$ and $\hat{a}_{\mathbf{q}}$ are the creation and annihilation operator of bosons with momentum $\mathbf{q}$, respectively. $g(t) = 4\pi\hbar^2 a_s(t)/m$ denotes the interaction strength, $\epsilon_{\mathbf{q}} = \hbar^2 q^2/(2m)$, where m is the atomic mass. N and V are the particle number and system volume, respectively. n_0 is the zero-momentum particle density. Now we define the generators as follows [14],

$$\hat{K}_0 = \frac{1}{2}\left(\hat{a}_{\mathbf{q}}^{\dagger}\hat{a}_{\mathbf{q}} + \hat{a}_{-\mathbf{q}}\hat{a}_{-\mathbf{q}}^{\dagger}\right); \quad (13)$$

$$\hat{K}_1 = \frac{1}{2}\left(\hat{a}_{\mathbf{q}}^{\dagger}\hat{a}_{-\mathbf{q}}^{\dagger} + \hat{a}_{\mathbf{q}}\hat{a}_{-\mathbf{q}}\right); \quad (14)$$

$$\hat{K}_2 = \frac{1}{2i}\left(\hat{a}_{\mathbf{q}}^{\dagger}\hat{a}_{-\mathbf{q}}^{\dagger} - \hat{a}_{\mathbf{q}}\hat{a}_{-\mathbf{q}}\right), \quad (15)$$

and the Casimir operator is written as $\hat{C} = \frac{1}{4}(\hat{a}_{\mathbf{q}}^{\dagger}\hat{a}_{\mathbf{q}} - \hat{a}_{-\mathbf{q}}^{\dagger}\hat{a}_{-\mathbf{q}}) - \frac{1}{4}$. In our case, $\hat{a}_{\mathbf{q}}^{\dagger}\hat{a}_{\mathbf{q}} = \hat{a}_{-\mathbf{q}}^{\dagger}\hat{a}_{-\mathbf{q}}$, and the good quantum number associated with $\hat{C}$ is $k = 1/2$. With the aid of Eqs.(13-15), the Bogoliubov Hamiltonian can be recast as

$$\hat{H}_{\text{Bog}}^{\mathbf{q}}(t) = 2\left[\epsilon_{\mathbf{q}} + g(t)n_0\right]\hat{K}_0 + g(t)n_0\left(\hat{K}_+ + \hat{K}_-\right). \quad (16)$$

As such, the approach presented in Section II is applicable to this system, and $\alpha(t) = 2\left[\epsilon_{\mathbf{q}} + g(t)n_0\right]$, $\beta(t) = 2g(t)n_0$. Substituting the expression of $\alpha(t)$ and $\beta(t)$ into Eqs. (8-10) and using the initial condition $\zeta_{\pm}(0) = 0, \eta(0) = 1$, we shall obtain the evolution operator at any time.

Considering the initial state in the experiment as a condensate at the zero momentum, we could geometrize the

dynamics on the Poincaré disk. Specifically, the initial state can be written as $|\psi_i\rangle = \left(\hat{a}_{\mathbf{q}=0}^\dagger\right)^N |0\rangle$ with N being the particle number. Then the time-dependent wave function becomes a coherent state

$$|\psi(t)\rangle = |\zeta_+(t), \frac{1}{2}\rangle = \left(1 - |\zeta_+(t)|^2\right)^{\frac{1}{2}} e^{\zeta_+(t)\hat{K}_+}|\psi_i\rangle, \quad (17)$$

which can be represented by a point on the Poincaré disk. Due to the pairwise interaction, the BEC is excited and the nonzero momentum particle number $\hat{N}_{\mathbf{q}} = \hat{K}_0 - \frac{1}{2}$ can be obtained straightforwardly

$$\langle\psi(t)|\hat{N}_{\mathbf{q}}|\psi(t)\rangle = \frac{1}{2}\left(\frac{1 + |\zeta_+(t)|^2}{1 - |\zeta_+(t)|^2}\right) - \frac{1}{2}. \quad (18)$$

In Fig.1, we present the dynamics of BEC under two different types of time-dependent interaction strength. In the first scheme, the interaction is sinusoidally oscillating with a frequency of ω, and after a few periods, say nT with $T = 2\pi/\omega$, the phase of $g(t)$ suddenly changes by π, as schematically plotted in Fig. 1(a1). We define the resonance mode via $\hbar^2 q_{\text{res}}^2/(2m) = \left(1/2 + 3\Delta^2/8\right)\hbar\omega$, where $\Delta = g_0 n_0/\hbar\omega$, and g_0 is the oscillation amplitude. The particle number $N_{\mathbf{q}}$ of the resonant mode increases exponentially at the early time. When the phase changes by π, $N_{\mathbf{q}}$ begins to decrease, and at $t = 2nT$, it drops to a small but nonzero value, as shown in Fig. 1(a2). On the contrary, in the second scheme, the interaction is turned off for a period of $T/2$ at $t = nT$, then oscillates again with the same phase, as schematically shown in Fig. 1(b1). It is found that at $t = (2n + 1/2)T$, $N_{\mathbf{q}}$ is vanishing small as shown in Fig. 1(b2), which means that BEC perfectly revives in the latter scheme.

These two schemes can be visualized on the Poincaré disk. Starting with the ground state of $\hat{K}_0$ means that the initial points is the disk center. The Hamiltonian in Eq.(12) is the linear combination of $\hat{K}_0$ and $\hat{K}_1$ that generate rotation and boost, respectively. Thus, the points represented the instant state on the disk will rotate around the disk center and move outwards to the boundary of the disk, as illustrated by the black curves in Fig. 1(a3) and (b3). In the first scheme, the point begins to rotate around and moves inwards to the center of the disk when the phase changes at $t = nT$. At $t = 2nT$, it does not stop at the center of the disk as shown in Fig. 1(a3), which indicates that the system does not revive. On the contrary, in the second scheme, when the interaction is turned off for a period of $T/2$, the point rotates by π around the center of the disk, indicated by the red curve in Figs. 1(b1-b3). Then it begins to rotate around and move towards the center. Finally, it goes back to the disk center, which implies that the system perfectly revives. For the non-resonant mode, the scheme above does not provide revivals as shown in Figs. 1(a4,a5,b4,b5). The revival requires a different waiting time when the interaction is turned off [29, 30].

B. Quantum dynamics in Scale-Invariant Fermi gas in harmonic trap

We consider the Fermi gas in 3D, and firstly focus on the two-body problems. For two fermions of spin $\uparrow$ and spin $\downarrow$ in harmonic potential with time-dependent trapping frequency, the free Hamiltonian is written as

$$\hat{H}_{2\text{b}}(t) = -\frac{\hbar^2}{2m}(\nabla_{\mathbf{r}_1}^2 + \nabla_{\mathbf{r}_2}^2) + \frac{1}{2}m\omega(t)^2(r_1^2 + r_2^2), \quad (19)$$

where m is the atomic mass, and $\omega(t)$ denotes the time-dependent trapping frequency. $\mathbf{r}_{1(2)}$ is the coordinate. We define the center of mass (CoM) and relative coordinates as $\mathbf{R} = (\mathbf{r}_1 + \mathbf{r}_2)/2$ and $\mathbf{r} = \mathbf{r}_1 - \mathbf{r}_2$, respectively. Here, we adopt the Bethe-Peierls boundary condition to incorporate the two-body interaction [35]

$$\psi(r_{ij} \to 0) \propto \frac{1}{r_{ij}} - \frac{1}{a_s}, \quad (20)$$

where a_s indicates the s-wave scattering length. $a_s \to 0$ and $a_s \to \infty$ correspond to non-interacting and unitary limit, respectively.

Due to the CoM Hamiltonian is not affected by the pairwise interaction, we focus on the relative motion, and the wave function is written as $\psi(\mathbf{r}, t)$. Since the angular momentum is conserved in this system, we could define a function $u(r, t) = r\phi(r, t)$ that solves Schrödinger equation $i\hbar\partial_t u(r, t) = \hat{H}u(r, t)$, where the time-dependent Hamiltonian is written as

$$\hat{H}(t) = -\frac{\hbar^2}{2\mu}\left[\frac{d^2}{dr^2} - \frac{\ell(\ell + 1)}{r^2}\right] + \frac{1}{2}\mu\omega(t)^2 r^2, \quad (21)$$

$\phi(r, t) = \psi(\mathbf{r}, t)/Y_{lm}(\theta, \varphi)$ is the radical wavefunction, μ is the reduced mass, and ℓ is the good quantum number of angular momentum. Now we define a set of generators as follows,

$$\hat{K}_0 \hbar\omega_0 = -\frac{\hbar^2}{4\mu}\left(\frac{\partial^2}{\partial r^2} - \frac{\ell(\ell + 1)}{r^2}\right) + \frac{1}{4}\mu\omega_0^2 r^2; \quad (22)$$

$$\hat{K}_1 \hbar\omega_0 = -\frac{\hbar^2}{4\mu}\left(\frac{\partial^2}{\partial r^2} - \frac{\ell(\ell + 1)}{r^2}\right) - \frac{1}{4}\mu\omega_0^2 r^2; \quad (23)$$

$$\hat{K}_2 \hbar\omega_0 = \frac{\hbar\omega_0}{2i}\left(r\frac{\partial}{\partial r} + \frac{1}{2}\right), \quad (24)$$

where $\omega_0 \equiv \omega(t_0)$ denotes the trapping frequency at $t = t_0$ with t_0 being the initial time.

It is straightforward to prove that the operators in Eqs. (22-24) satisfy the commutation relation of the $SU(1,1)$ generators, and the Casimir operator is written as $\hat{C} = \ell(\ell + 1)/4 - 3/16$. For the s-wave case $(\ell = 0)$, the good quantum number for the Casimir is $k = 3/4$ or $k = 1/4$. They are the ground state energy of $\hat{K}_0 \hbar\omega_0$ in Eq.(22) without interaction or with unitary interaction, respectively. To be specific, (I): for $k = 3/4$, $u_{\text{fr}}(r) \propto re^{-\mu\omega_0 r^2/(2\hbar)}$ solves $\hat{K}_0 u_{\text{fr}}(r) = (3/4)u_{\text{fr}}(r)$ under the boundary condition $u_{\text{fr}}(r \to \infty) \to 0$. As such,

in the limit of $r \to 0$, $\frac{u_{\mathrm{fr}}(r)}{r} \to 1 + \mathcal{O}(r^2)$, which is the short range boundary condition of two non-interacting particles. (II): for $k = 1/4$, $u_{\mathrm{int}}(r) \propto e^{-\mu\omega_0 r^2/(2\hbar)}$ solves $\hat{K}_0 u_{\mathrm{int}}(r) = (1/4)u_{\mathrm{int}}(r)$ under the boundary condition $u_{\mathrm{int}}(r \to \infty) \to 0$. In the limit of $r \to 0$, we have $\frac{u_{\mathrm{int}}(r)}{r} \to \frac{1}{r} + \mathcal{O}(r)$, which is short range boundary of two particles with unitary interaction. As a result, case (I) and (II) correspond to non-interacting and unitary interacting Fermi gas in a harmonic trap with frequency of ω_0, respectively. For both cases, the interaction, that can be simulated by the pseudo-potential $(4\pi\hbar^2 a_s/m)\delta(\mathbf{r})\partial_r r$ [36], is invariant under scale transformation $r \to \Omega r$ with Ω being an arbitrary real number. As a result, scale-invariant Fermi gas refers to that without interaction or with unitary interaction.

Now we consider the quantum dynamics of the scale-invariant Fermi gas. To this end, we firstly recast the Hamiltonian in Eq.(21) as

$$\frac{\hat{H}(t)}{\hbar\omega_0} = \left(1 + \frac{\omega(t)^2}{\omega_0^2}\right)\hat{K}_0 + \left(1 - \frac{\omega(t)^2}{\omega_0^2}\right)\hat{K}_1. \quad (25)$$

The generic approach for the quantum dynamics in Section II then is applicable to this system with $\alpha(t) = 1 + \omega(t)^2/\omega_0^2$ and $\beta(t) = 1 - \omega(t)^2/\omega_0^2$. Substituting $\alpha(t)$ and $\beta(t)$ into Eqs.(8-10) and imposing the initial condition $\zeta_\pm(0) = 0, \eta(0) = 1$, we can obtain the evolution operator $\hat{U}(t,0)$. If the initial state were $\phi_i(r) = \frac{u_{\mathrm{fr}}(r)}{r}$ or $\frac{u_{\mathrm{int}}(r)}{r}$, the time-dependent wave function then is written as

$$\phi(r,t) = \eta(t)^{\frac{3(1)}{4}} e^{\zeta_+(t)\hat{K}_+}\phi_i(r), \quad (26)$$

and the quantum dynamics can be visualized on the Poincaré disk characterized by ζ_+. For the case that the initial state is not the ground state of $\hat{K}_0$, but the ground state of system with trapping frequency $\tilde{\omega}_0$, the initial states for the noninteracting and unitary gas can be obtained by a dilation

$$r\tilde{\phi}_i(r) = e^{-i\theta\hat{K}_2}u_{\mathrm{fr(int)}}(r) \quad (27)$$

with $\theta = \ln(\omega_0/\tilde{\omega}_0)$. Then the time-dependent wave function can be obtained

$$\begin{aligned} r\phi(r,t) &= \hat{U}(t,0)e^{-i\theta\hat{K}_2}u_{\mathrm{fr(int)}}(r) \\ &= e^{\tilde{\zeta}_+(t)\hat{K}_+}e^{\hat{K}_0 \ln \tilde{\eta}(t)}e^{\tilde{\zeta}_-(t)\hat{K}_-}u_{\mathrm{fr(int)}}(r) \\ &= \tilde{\eta}(t)^{\frac{3(1)}{4}} e^{\tilde{\zeta}_+(t)\hat{K}_+}u_{\mathrm{fr(int)}}(r), \end{aligned} \quad (28)$$

where $\hat{U}(t,0)$ is the evolution operator defined in Eq.(5). To prove the second line, we have used the Baker-Campbell-Hausdorff formula. A straightforward algebra

shows that

$$\tilde{\zeta}_+(t) = \frac{\zeta_+(t)\cosh\frac{\theta}{2} - [\eta(t) - \zeta_-(t)\zeta_+(t)]\sinh\frac{\theta}{2}}{\cosh\frac{\theta}{2} + \zeta_-(t)\sinh\frac{\theta}{2}}; \quad (29)$$

$$\tilde{\zeta}_-(t) = \frac{\zeta_-(t)\cosh\frac{\theta}{2} + \sinh\frac{\theta}{2}}{\cosh\frac{\theta}{2} + \zeta_-(t)\sinh\frac{\theta}{2}}; \quad (30)$$

$$\sqrt{\tilde{\eta}(t)} = \frac{\sqrt{\eta(t)}}{\cosh\frac{\theta}{2} + \zeta_-(t)\sinh\frac{\theta}{2}}. \quad (31)$$

For details, please refer to Appendix B. As a result, if the initial state is not the ground state of $\hat{K}_0$, the dynamic of scale-invariant Fermi gas can be visualized on the Poincaré disk that is characterized by $\tilde{\zeta}_+$, instead of ζ_+. From Eqs.(29-31), we see that (1): when $\theta = 0$, i.e., $\tilde{\omega}_0 = \omega_0$, $\tilde{\zeta}_\pm(t) = \zeta_\pm(t)$ and $\tilde{\eta}_\pm(t) = \eta_\pm(t)$; (2): at the initial time $t = 0$, $\tilde{\zeta}_\pm(0) = \mp\tanh(\theta/2)$ and $\tilde{\eta}(0) = 1/\cosh(\theta/2)$. Before further proceeding, an intuitive physical picture will be helpful. $\tilde{\omega}_0 = \omega_0$ means that the initial state is the ground state of the initial harmonic trap, while $\tilde{\omega}_0 > (<)\omega_0$ means that the ground state size of the initial harmonic trap is larger(smaller) than the initial state size.

By expressing the time-dependent wavefunction in terms of $SU(1,1)$ coherent state, we can obtain the expectation value of $\hat{r}^2$

$$\begin{aligned} \langle\hat{r}^2\rangle_{\mathrm{fr(int)}}(t) &= \left\langle \tilde{\zeta}_+(t), \frac{1(3)}{4} \middle| \hat{r}^2 \middle| \tilde{\zeta}_+(t), \frac{1(3)}{4} \right\rangle \\ &= \frac{2}{\mu\omega_0^2}\left\langle \tilde{\zeta}_+(t), \frac{1(3)}{4} \middle| \hat{K}_0 - \hat{K}_1 \middle| \tilde{\zeta}_+(t), \frac{1(3)}{4} \right\rangle \\ &= \frac{3(1)}{2}\frac{\hbar}{\mu\omega_0}\frac{1 + |\tilde{\zeta}_+(t)|^2 - 2\Re[\tilde{\zeta}_+(t)]}{1 - |\tilde{\zeta}_+(t)|^2}. \end{aligned} \quad (32)$$

At the initial time $t = 0$, $\langle\hat{r}^2\rangle_{\mathrm{fr(int)}}(0) = \frac{3(1)}{2}\frac{\hbar}{\mu\tilde{\omega}_0}$ characterizes the cloud size in a harmonic trap of frequency $\tilde{\omega}_0$. Since the interaction does not affect the CoM motion, the CoM wave function will always be of free form with $k = 3/4$. Following the same derivation, we have

$$\frac{\langle\hat{R}^2\rangle(t)}{\langle\hat{R}^2\rangle(0)} = \frac{\tilde{\omega}_0}{\omega_0}\frac{1 + |\tilde{\zeta}_+(t)|^2 - 2\Re[\tilde{\zeta}_+(t)]}{1 - |\tilde{\zeta}_+(t)|^2}. \quad (33)$$

It is obvious that the CoM and relative motion have the same dynamical behavior. As such, we conclude that the cloud size as a function of time will also obey Eq.(33). We would like to point out that our approach can be applied to the study of dynamics under arbitrary form of $\omega(t)$ and particle number. The expectation values for observables that are expressed as $\hat{K}_-^v \hat{K}_0^w \hat{K}_+^p$ can be readily obtained, where v, w, p are arbitrary non-negative integers [37].

Now we consider a special case that the time-dependent trapping frequency is $\omega(t) = 1/(\sqrt{\lambda}t)$ with λ being a dimensionless parameter. We denote the initial time as t_0 and use initial frequency $\omega(t_0)$ to define the generators in Eqs.(22-24), i.e., $\omega_0 = \omega(t_0)$. In Fig. 2,
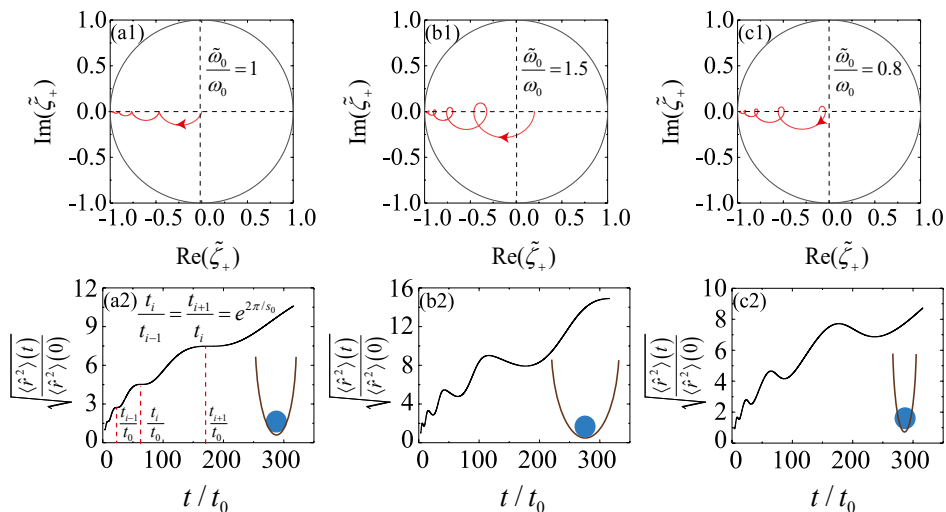
FIG. 2. Quantum dynamics of scale-invariant Fermi gas induced by the time-dependent harmonic trap. The frequency varies as $\omega(t) = 1/(\sqrt{\lambda}t)$. (a1,a2): The initial state is the ground state of the initial Hamiltonian. On the Poincaré disk, the starting point locates at the center of the disk, and $\langle \hat{r}^2 \rangle(t)$ exhibit a discrete scaling law. (b1,b2): The initial state is in a loosely confined harmonic potential. The starting point is not the center of the disk, and the discrete scaling law disappears. (c1,c2): The initial state is in a tightly confined harmonic potential. Similar to the previous case, the starting point is not the center of the disk and the discrete scaling law disappears. Here $\tilde{\zeta}_+$ is dimensionless.

we illustrate the quantum dynamics starting with different initial Hamiltonians and the visualization of quantum dynamics on the Poincaré disk characterized by $\tilde{\zeta}_+$. When the initial state is the ground state of the initial harmonic trap, i.e., $\tilde{\omega}_0 = \omega_0$, our results show that the cloud size expands when the trapping frequency becomes smaller. Moreover, a series of plateaus appear for $\langle \hat{r}^2 \rangle(t)$, the corresponding times of which obey a discrete scaling law $t_{i+1}/t_i = e^{2\pi/s_0}$ with $s_0 = \sqrt{4/\lambda - 1}$, as shown in Fig. 2(a). This phenomenon has been observed and named as "Efimovian expansion" [10]. On the Poincaré disk, the dynamics trajectory forms a series of similar semicircles, and the initial point is the disk center. The ending point locates at the boundary of the disk, which implies that the cloud size becomes infinitely large. When the initial state is not the ground state of the initial harmonic trap, that is, the ground state size of the initial harmonic trap is either smaller ($\omega_0 > \tilde{\omega}_0$) or larger ($\omega_0 < \tilde{\omega}_0$) than the initial state size, the expectation value $\langle \hat{r}^2 \rangle$ grows. But on top of the profile a series of local minima instead of plateaus appears. The discrete scaling law also disappears, as shown in Figs. 2(b,c). On the Poincaré disk, the dynamics trajectory forms a string-like shape. The starting point is not the disk center. This is due to the fact that the starting point for these two cases is related to the disk center by a dilation $e^{-i\theta \hat{K}_2}$. The ending points also locate at the boundary of the disk, the same as the former case.

IV. QUANTUM DYNAMICS IN OSCILLATING OPTICAL LATTICE

In the previous two sections, we have investigated the quantum dynamics induced by a time-dependent interaction strength and an external trapping potential. For cold atoms in an optical lattice, the effective mass is modified by the distorted dispersion. Considering Bose gas condensed at the bottom of the s-band, the effective mass can be written as

$$m_i^* = \hbar^2 \left(\frac{\partial^2 \epsilon_{\mathbf{q}}}{\partial q_i^2} \right)^{-1} \Bigg|_{q_i=0}, \; i = x, y, z, \qquad (34)$$

where $\epsilon_{\mathbf{q}}$ denotes the dispersion. For the tight binding model, we have $\epsilon_{\mathbf{q}} = -\sum_{i=x,y,z} t_i \cos(q_i a)$ with t_i being the tunneling strength along the i-direction. Since t_i is determined by the lattice depth that can be manipulated time-dependently, the dispersion varies for different lattice depth, and so does the effective mass $m_i^*(t)$ [38]. Similar to the case in Sec III, we consider the Bose gases with weak interaction, and the system is described by the Bogoliubov Hamiltonian that can be written as [26, 30]

$$\hat{H}_{\text{Bog}}^{\mathbf{q}}(t) = \frac{1}{2} \left(\frac{\hbar^2 q^2}{2m^*(t)} + gn_0 \right) \left(\hat{a}_{\mathbf{q}}^\dagger \hat{a}_{\mathbf{q}} + \hat{a}_{-\mathbf{q}} \hat{a}_{-\mathbf{q}}^\dagger \right)$$
$$+ \frac{gn_0}{2} \left(\hat{a}_{\mathbf{q}}^\dagger \hat{a}_{-\mathbf{q}}^\dagger + \hat{a}_{\mathbf{q}} \hat{a}_{-\mathbf{q}} \right), \qquad (35)$$

then we define $\alpha(t) = \frac{\hbar^2 q^2}{m^*(t)} + 2gn_0$, and $\beta(t) = 2gn_0$. Upon substituting $\alpha(t)$ and $\beta(t)$ into Eqs. (8-10), the dynamics of our system can be obtained.

Here we assume that the optical lattice depth varies as $V(t) = V_0 \sin^2(\omega t)$. As such, the kinetic energy can
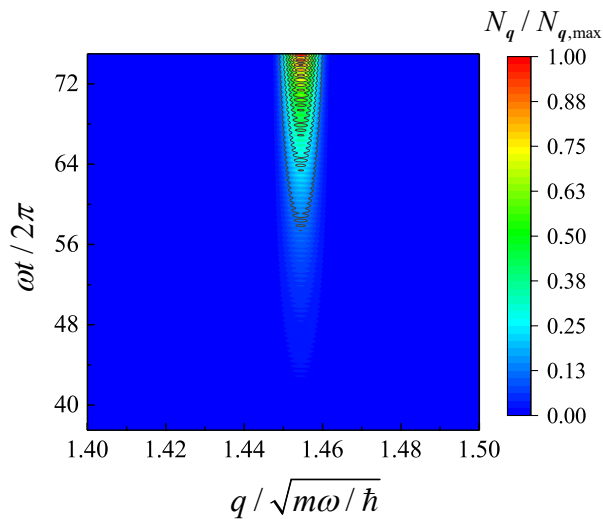
FIG. 3. Quantum dynamics of Bose gas in an oscillating optical lattice. Only the particles near the resonant mode are excited. In our calculation, we set $gn_0=0.1\hbar\omega$. The color bar represents the normalized particle number $N_q/N_{\mathbf{q},\max}$ in the $\mathbf{q}$-mode, where $N_{\mathbf{q},\max}$ is the maximum of $N_{\mathbf{q}}$ for the resonant mode.

FIG. 4. Interaction effect on the resonant mode. The interaction enhances the excitation of the resonant mode. Inset: The interaction shifts the resonant mode toward the lower momentum. In our calculation, we take shot for the particle number $N_{\mathbf{q}}$ at $t = 50T$. V_0 denotes the lattice depth at the beginning and E_R is the recoil energy. $N_{\mathbf{q},\max}$ is the maximum of particle number for $gn_0 = 0.16\hbar\omega$ at $t = 50T$.

be obtained by exact diagonalization, and varies with a single frequency. Then the time-dependent effective mass can be obtained via Eq.(34). V_0 denotes the maximal lattice depth and $E_R =\hbar^2\pi^2/(2ma^2)$ is the recoil energy, m is the mass of the particle and a is half the wavelength. Similar to Eq.(18), the particle number of the $\mathbf{q}$-mode can be readily obtained. In Fig. 3, we present particle number with nonzero momentum as a function of evolution time. It is clear that only a particular mode $q_{\rm res} \approx 1.455\sqrt{m\omega/\hbar}$ is excited by the oscillation, where $q_{\rm res}$ is defined as the resonance mode via $\hbar^2q_{\rm res}^2/(2\bar{m}^*) = n\hbar\omega$. $\bar{m}^*$ denotes the mean value of the varying effective mass, and n is an integer. Here we have shown the case of $n = 1$, and the resonant mode with $n \geq 2$ can also be observed but with a decreased strength.

In addition, we have also studied the interaction effect on the resonant mode. We only consider the weak interaction, and the mean-field Bogoliubov theory holds. As illustrated in Fig. 4, our results show that (1): The stronger the interaction is, the more particles are excited in the resonant mode, which makes sense by referring to Eq.(35). (2): When the interaction strength increases, the resonant mode moves towards the lower momentum, as shown in the inset. Similar results also exist for the resonant mode with $n \geq 2$.

V. CONCLUSION & OUTLOOK

In summary, we studied the quantum dynamics of the system with the $SU(1,1)$ symmetry. Instead of performing the time-ordering evolution, the dynamics can be obtained by solving a set of algebraic equations. The evo-

lution operator can be expressed as an element of the $SU(1,1)$ group, so that the wave function can be visualized on the Poincaré disk, a prototype of the hyperbolic surface. Taking Bose and scale-invariant Fermi gas as examples, we demonstrate this approach. Our method can readily reproduce the previous results. The dynamics of BEC and scaling invariant Fermi gas are studied. The revival of BEC and Efimovian expansion can be obtained in a simpler way. We also provide an intuitive geometric picture of various quantum dynamical systems, that is, the dynamics can be visualised on a Poincaré disk. The quantum dynamics of Bose gas in oscillating optical lattice have also been studied. In this system, the effective mass is time-dependent and the resonant mode is determined by the mean value of the effective mass. The interaction effect on the resonant mode is also studied.

We would like to point out that our method can also be implemented to the few-body system, such as the study of the dynamics in the three-body problem [39–41]. By characterizing how strong the broken of the $SU(1,1)$ symmetry is, our method may also be applied to study the quantum anomaly [42–47]. For instance, for three identical bosons in a harmonic trap, the Hamiltonian can be expressed by generators of $SU(1,1)$ group. While the dynamics is predicted by Eqs. (8-10), the short range boundary condition breaks the $SU(1,1)$ symmetry and leads to the deviation from the predicted trajectory. Since our method does not depend on the configuration of the spatial confinement, it can also be implemented to the study of the parametric excitation in BEC [48] or the quantum enhanced sensing [49].

ACKNOWLEDGMENTS

Appendix A: Derivation of Eqs.(8-10)

In this appendix, we show the detailed derivation of the Eqs.(8-10) in the main text. The evolution operator satisfies the following equation

$$\frac{\partial_t \hat{U}(t,0)}{\hat{U}(t,0)} = -i\alpha(t)\hat{K}_0 - \frac{i}{2}\beta(t)(\hat{K}_+ + \hat{K}_-). \tag{A1}$$

Since the commutation relations of $K_{0,1,2}$ are closed, we can express the evolution operator in the normal-ordered form

$$\hat{U}(t,0) = e^{\zeta_+(t)\hat{K}_+} e^{\hat{K}_0 \ln \eta(t)} e^{\zeta_-(t)\hat{K}_-}, \tag{A2}$$

which means

$$\partial_t \hat{U}(t,0) = \frac{\partial \zeta_+(t)}{\partial t} \hat{K}_+ e^{\zeta_+(t)\hat{K}_+} e^{\hat{K}_0 \ln \eta(t)} e^{\zeta_-(t)\hat{K}_-}$$
$$+ \eta(t)^{-1} \frac{\partial \eta(t)}{\partial t} e^{\zeta_+(t)\hat{K}_+} \hat{K}_0 e^{\hat{K}_0 \ln \eta(t)} e^{\zeta_-(t)\hat{K}_-}$$
$$+ \frac{\partial \zeta_-(t)}{\partial t} e^{\zeta_+(t)\hat{K}_+} e^{\hat{K}_0 \ln \eta(t)} \hat{K}_- e^{\zeta_-(t)\hat{K}_-}. \tag{A3}$$

For further proceeding, we need to calculate

$$g_1(t) = e^{\zeta_+(t)\hat{K}_+} \hat{K}_0, \tag{A4}$$
$$g_2(t) = e^{\hat{K}_0 \ln \eta(t)} \hat{K}_-, \tag{A5}$$
$$g_3(t) = e^{\zeta_+(t)\hat{K}_+} \hat{K}_-. \tag{A6}$$

To be specific, it is straightforward to prove the following identity

$$\frac{dg_1(t)}{dt} = e^{\zeta_+(t)\hat{K}_+} \hat{K}_+ \hat{K}_0 = e^{\zeta_+(t)\hat{K}_+}(\hat{K}_0 \hat{K}_+ - \hat{K}_+)$$
$$= g_1(t)\hat{K}_+ - e^{\zeta_+(t)\hat{K}_+} \hat{K}_+. \tag{A7}$$

Under the initial condition that $g_1(0) = \hat{K}_0$, we find

$$g_1(t) = (\hat{K}_0 - \zeta_+(t)\hat{K}_+)e^{\zeta_+(t)\hat{K}_+}. \tag{A8}$$

Utilizing the same method, we have

$$g_2(t) = \eta(t)^{-1} \hat{K}_- e^{\hat{K}_0 \ln \eta(t)}. \tag{A9}$$

and

$$g_3(t) = \left[\hat{K}_- - 2\zeta_+(t)\hat{K}_0 + \zeta_+(t)^2 \hat{K}_+ \right] e^{\zeta_+(t)\hat{K}_+}. \tag{A10}$$

As a result, we have

$$\frac{\partial_t \hat{U}(t,0)}{\hat{U}(t,0)} = \frac{\partial \zeta_+(t)}{\partial t} \hat{K}_+ + \eta(t)^{-1} \frac{\partial \eta(t)}{\partial t} \left[\hat{K}_0 - \zeta_+(t)\hat{K}_+ \right]$$
$$+ \eta(t)^{-1} \frac{\partial \zeta_-(t)}{\partial t} \left[\hat{K}_- - 2\zeta_+(t)\hat{K}_0 + \zeta_+(t)^2 \hat{K}_+ \right]$$
$$= \left[\frac{\partial \zeta_+(t)}{\partial t} - \frac{\zeta_+(t)}{\eta(t)} \frac{\partial \eta(t)}{\partial t} + \frac{\zeta_+(t)^2}{\eta(t)} \frac{\partial \zeta_-(t)}{\partial t} \right] \hat{K}_+$$
$$+ \frac{1}{\eta(t)} \left[\frac{\partial \eta(t)}{\partial t} - 2\zeta_+(t)\frac{\partial \zeta_-(t)}{\partial t} \right] \hat{K}_0 + \frac{1}{\eta(t)} \frac{\partial \zeta_-(t)}{\partial t} \hat{K}_-. \tag{A11}$$

Comparing with Eq.(A1), we obtain Eqs.(8-10) in the main text,

$$-i\alpha(t) = \frac{1}{\eta(t)} \left[\frac{\partial \eta(t)}{\partial t} - 2\zeta_+(t)\frac{\partial \zeta_-(t)}{\partial t} \right]; \tag{A12}$$

$$-\frac{i}{2}\beta(t) = \frac{\partial \zeta_+(t)}{\partial t} - \frac{\zeta_+(t)}{\eta(t)} \frac{\partial \eta(t)}{\partial t} + \frac{\zeta_+(t)^2}{\eta(t)} \frac{\partial \zeta_-(t)}{\partial t}; \tag{A13}$$

$$-\frac{i}{2}\beta(t) = \frac{1}{\eta(t)} \frac{\partial \zeta_-(t)}{\partial t}. \tag{A14}$$

Appendix B: Derivation of Eqs.(29-31)

In this part, we present a detailed derivation for Eqs.(29-31) in the main text. To this end, we choose the non-unitary representation of the $SU(1,1)$ group. Specifically, $\hat{K}_0 = \hat{\sigma}_0/2$ and $\hat{K}_\pm = i\hat{\sigma}_\pm = i(\hat{\sigma}_1 \pm i\hat{\sigma}_2)/2$. $\sigma_{0,1,2}$ are Pauli matrices. It can be readily checked that this definition satisfies the communation relation of the $SU(1,1)$ algebra. Then the operator in Eq.(28) can be rewritten as

$$\hat{U}(t,0)e^{-i\theta \hat{K}_2} = e^{\zeta_+(t)\hat{K}_+}e^{\hat{K}_0 \ln \eta(t)}e^{\zeta_-(t)\hat{K}_-}e^{-i\theta \hat{K}_2} = e^{\zeta_+(t)i\hat{\sigma}_+}e^{\ln \eta(t)\hat{\sigma}_0/2}e^{\zeta_-(t)i\hat{\sigma}_-}e^{\theta \hat{\sigma}_2/2}$$

$$= \frac{1+\hat{\sigma}_0}{2}\left[\frac{[\eta(t)-\zeta_-(t)\zeta_+(t)]\cosh\frac{\theta}{2} - \zeta_+(t)\sinh\frac{\theta}{2}}{\sqrt{\eta(t)}}\right] + \frac{1-\hat{\sigma}_0}{2}\left[\frac{\cosh\frac{\theta}{2}+\zeta_-(t)\sinh\frac{\theta}{2}}{\sqrt{\eta(t)}}\right]$$

$$+ i\hat{\sigma}_+\left[\frac{\zeta_+(t)\cosh\frac{\theta}{2} - [\eta(t)-\zeta_-(t)\zeta_+(t)]\sinh\frac{\theta}{2}}{\sqrt{\eta(t)}}\right] + i\hat{\sigma}_-\left[\frac{\zeta_-(t)\cosh\frac{\theta}{2} + \sinh\frac{\theta}{2}}{\sqrt{\eta(t)}}\right] \qquad (B1)$$

Using the same representation, we have

$$e^{\tilde{\zeta}_+(t)\hat{K}_+}e^{\hat{K}_0 \ln \tilde{\eta}(t)}e^{\tilde{\zeta}_-(t)\hat{K}_-} = e^{\tilde{\zeta}_+(t)i\hat{\sigma}_+}e^{\ln \eta(t)\hat{\sigma}_0/2}e^{\zeta_-(t)i\hat{\sigma}_-}$$

$$= \frac{1+\hat{\sigma}_0}{2}\frac{\tilde{\eta}(t)-\tilde{\zeta}_+(t)\tilde{\zeta}_-(t)}{\sqrt{\tilde{\eta}(t)}} + \frac{1-\hat{\sigma}_0}{2}\frac{1}{\sqrt{\tilde{\eta}(t)}} + \tilde{\zeta}_+(t)\tilde{\eta}(t)^{-1/2}i\hat{\sigma}_+ + \tilde{\zeta}_-(t)\tilde{\eta}(t)^{-1/2}i\hat{\sigma}_-$$

$$+ \hat{\sigma}_0\left[\sinh\frac{\ln \tilde{\eta}(t)}{2} - \frac{1}{2}\tilde{\zeta}_+(t)\tilde{\zeta}_-(t)\tilde{\eta}(t)^{-1/2}\right] \qquad (B2)$$

As a result, by comparing the respective terms in Eq.(B1) and Eq.(B2), we find

$$\frac{1}{\sqrt{\tilde{\eta}(t)}} = \frac{\cosh\frac{\theta}{2}+\zeta_-(t)\sinh\frac{\theta}{2}}{\sqrt{\eta(t)}}; \qquad (B3)$$

$$\frac{\tilde{\zeta}_+(t)}{\sqrt{\tilde{\eta}(t)}} = \frac{\zeta_+(t)\cosh\frac{\theta}{2} - [\eta(t)-\zeta_-(t)\zeta_+(t)]\sinh\frac{\theta}{2}}{\sqrt{\eta(t)}}; \qquad (B4)$$

$$\frac{\tilde{\zeta}_-(t)}{\sqrt{\tilde{\eta}(t)}} = \frac{\zeta_-(t)\cosh\frac{\theta}{2} + \sinh\frac{\theta}{2}}{\sqrt{\eta(t)}}. \qquad (B5)$$

After some straightforward algebra, we obtain Eqs.(29-31) in the main text,

$$\tilde{\zeta}_+(t) = \frac{\zeta_+(t)\cosh\frac{\theta}{2} - [\eta(t)-\zeta_-(t)\zeta_+(t)]\sinh\frac{\theta}{2}}{\cosh\frac{\theta}{2}+\zeta_-(t)\sinh\frac{\theta}{2}}; \qquad (B6)$$

$$\tilde{\zeta}_-(t) = \frac{\zeta_-(t)\cosh\frac{\theta}{2} + \sinh\frac{\theta}{2}}{\cosh\frac{\theta}{2}+\zeta_-(t)\sinh\frac{\theta}{2}}; \qquad (B7)$$

$$\sqrt{\tilde{\eta}(t)} = \frac{\sqrt{\eta(t)}}{\cosh\frac{\theta}{2}+\zeta_-(t)\sinh\frac{\theta}{2}}. \qquad (B8)$$

[1] I. Bloch, J. Dalibard, and W. Zwerger, Many-body physics with ultracold gases, Rev. Mod. Phys. **80**, 885 (2008).

[2] C. Chin, R. Grimm, P. Julienne, and E. Tiesinga, Feshbach resonances in ultracold gases, Rev. Mod. Phys. **82**, 1225 (2010).

[3] L. W. Clark, A. Gaj, L. Feng, and C. Chin, Collective emission of matter-wave jets from driven bose–einstein condensates, Nature **551**, 356 (2017).

[4] J. Hu, L. Feng, Z. Zhang, and C. Chin, Quantum simulation of unruh radiation, Nature Physics **15**, 785 (2019).

[5] E. M. Wright, T. Wong, M. J. Collett, S. M. Tan, and D. F. Walls, Collapses and revivals in the interference between two bose-einstein condensates formed in small atomic samples, Phys. Rev. A **56**, 591 (1997).

[6] I. Gotlibovych, T. F. Schmidutz, A. L. Gaunt, N. Navon, R. P. Smith, and Z. Hadzibabic, Observing properties of an interacting homogeneous bose-einstein condensate: Heisenberg-limited momentum spread, interaction energy, and free-expansion dynamics, Phys. Rev. A **89**, 061604 (2014).

[7] M. Aidelsburger, J. L. Ville, R. Saint-Jalm, S. Nascimbène, J. Dalibard, and J. Beugnon, Relaxation dynamics in the merging of n independent condensates, Phys. Rev. Lett. **119**, 190403 (2017).

[8] J. L. Ville, T. Bienaimé, R. Saint-Jalm, L. Corman, M. Aidelsburger, L. Chomaz, K. Kleinlein, D. Perconte, S. Nascimbène, J. Dalibard, and J. Beugnon, Loading and compression of a single two-dimensional bose gas in an optical accordion, Phys. Rev. A **95**, 013632 (2017).

[9] R. Saint-Jalm, P. C. M. Castilho, E. Le Cerf, B. Bakkali-Hassani, J.-L. Ville, S. Nascimbene, J. Beugnon, and J. Dalibard, Dynamical symmetry and breathers in a two-dimensional bose gas, Phys. Rev. X **9**, 021035 (2019).

[10] S. Deng, Z.-Y. Shi, P. Diao, Q. Yu, H. Zhai, R. Qi, and H. Wu, Observation of the efimovian expansion in scale-invariant fermi gases, Science **353**, 371 (2016).

[11] S. Deng, P. Diao, F. Li, Q. Yu, S. Yu, and H. Wu, Observation of dynamical super-efimovian expansion in a unitary fermi gas, Phys. Rev. Lett. **120**, 125301 (2018).

[12] Z.-Y. Shi, R. Qi, H. Zhai, and Z. Yu, Dynamic super efimov effect, Phys. Rev. A **96**, 050702 (2017).

[13] B. Yurke, S. L. McCall, and J. R. Klauder, Su(2) and su(1,1) interferometers, Phys. Rev. A **33**, 4033 (1986).

[14] M. Novaes, Some basics of su(1,1), Revista Brasileira de Ensino de Fsica **26**, 351 (2004).

[15] F. Werner and Y. Castin, Unitary gas in an isotropic harmonic trap: Symmetry properties and applications, Phys. Rev. A **74**, 053604 (2006).

[16] P. K. Aravind, Pseudospin approach to the dynamics and squeezing of su(2) and su(1, 1) coherent states, J. Opt. Soc. Am. B **5**, 1545 (1988).

[17] N. Balazs and A. Voros, Chaos on the pseudosphere, Physics Reports **143**, 109 (1986).

[18] F. Chevy, V. Bretin, P. Rosenbusch, K. W. Madison, and J. Dalibard, Transverse breathing mode of an elongated bose-einstein condensate, Phys. Rev. Lett. **88**, 250402 (2002).

[19] L. P. Pitaevskii and A. Rosch, Breathing modes and hidden symmetry of trapped atoms in two dimensions, Phys. Rev. A **55**, R853 (1997).

[20] E. Vogt, M. Feld, B. Fröhlich, D. Pertot, M. Koschorreck, and M. Köhl, Scale invariance and viscosity of a two-dimensional fermi gas, Phys. Rev. Lett. **108**, 070404 (2012).

[21] C. Gao and Z. Yu, Breathing mode of two-dimensional atomic fermi gases in harmonic traps, Phys. Rev. A **86**, 043609 (2012).

[22] J. Hofmann, Quantum anomaly, universal relations, and breathing mode of a two-dimensional fermi gas, Phys. Rev. Lett. **108**, 185303 (2012).

[23] H. Hu and X.-J. Liu, Resonantly interacting p-wave fermi superfluid in two dimensions: Tan's contact and the breathing mode, Phys. Rev. A **100**, 023611 (2019).

[24] Y.-C. Zhang and S. Zhang, Strongly interacting p-wave fermi gas in two dimensions: Universal relations and breathing mode, Phys. Rev. A **95**, 023603 (2017).

[25] U. Toniolo, B. C. Mulkerin, X.-J. Liu, and H. Hu, Breathing-mode frequency of a strongly interacting fermi gas across the two- to three-dimensional crossover, Phys. Rev. A **97**, 063622 (2018).

[26] Y.-Y. Chen, P. Zhang, W. Zheng, Z. Wu, and H. Zhai, Many-body echo, Phys. Rev. A **102**, 011301 (2020).

[27] Y. Cheng and Z.-Y. Shi, Many-body dynamics with time-dependent interaction, Phys. Rev. A **104**, 023307 (2021).

[28] P. Zhang and Y. Gu, Periodically and Quasi-periodically Driven Dynamics of Bose-Einstein Condensates, SciPost Phys. **9**, 79 (2020).

[29] C. Lyu, C. Lv, and Q. Zhou, Geometrizing quantum dynamics of a bose-einstein condensate, Phys. Rev. Lett. **125**, 253401 (2020).

[30] C. Lv, R. Zhang, and Q. Zhou, $su(1,1)$ echoes for breathers in quantum gases, Phys. Rev. Lett. **125**, 253002 (2020).

[31] M. Ban, Decomposition formulas for su(1, 1) and su(2)

lie algebras and their applications in quantum optics, J. Opt. Soc. Am. B **10**, 1347 (1993).

[32] S. Will, From Atom Optics to Quantum Simulation (From Atom Optics to Quantum Simulation, 2013).

[33] E. L. Hahn, Spin echoes, Phys. Rev. **80**, 580 (1950).

[34] H. Y. Carr and E. M. Purcell, Effects of diffusion on free precession in nuclear magnetic resonance experiments, Phys. Rev. **94**, 630 (1954).

[35] H. Bethe and R. Peierls, Quantum theory of the diplon, Proceedings of the Royal Society of London. Series A - Mathematical and Physical Sciences **148**, 146 (1935).

[36] K. Huang and C. N. Yang, Quantum-mechanical many-body problem with hard-sphere interaction, Phys. Rev. **105**, 767 (1957).

[37] T. Lisowski, Expectation values of squeezing hamiltonians in the SU(1,1) coherent states, Journal of Physics A: Mathematical and General **25**, L1295 (1992).

[38] A. Eckardt, Colloquium: Atomic quantum gases in periodically driven optical lattices, Rev. Mod. Phys. **89**, 011004 (2017).

[39] D. S. Petrov, The few-atom problem, (2012), arXiv:1206.5752 [cond-mat.quant-gas].

[40] P. Naidon and S. Endo, Efimov physics: a review, Reports on Progress in Physics **80**, 056001 (2017).

[41] C. H. Greene, P. Giannakeas, and J. Pérez-Ríos, Universal few-body physics and cluster formation, Rev. Mod. Phys. **89**, 035006 (2017).

[42] K. Merloti, R. Dubessy, L. Longchambon, M. Olshanii, and H. Perrin, Breakdown of scale invariance in a quasi-two-dimensional bose gas due to the presence of the third dimension, Phys. Rev. A **88**, 061603 (2013).

[43] E. Elliott, J. A. Joseph, and J. E. Thomas, Observation of conformal symmetry breaking and scale invariance in expanding fermi gases, Phys. Rev. Lett. **112**, 040405 (2014).

[44] M. Holten, L. Bayha, A. C. Klein, P. A. Murthy, P. M. Preiss, and S. Jochim, Anomalous breaking of scale invariance in a two-dimensional fermi gas, Phys. Rev. Lett. **121**, 120401 (2018).

[45] T. Peppler, P. Dyke, M. Zamorano, I. Herrera, S. Hoinka, and C. J. Vale, Quantum anomaly and 2d-3d crossover in strongly interacting fermi gases, Phys. Rev. Lett. **121**, 120402 (2018).

[46] H. Hu, B. C. Mulkerin, U. Toniolo, L. He, and X.-J. Liu, Reduced quantum anomaly in a quasi-two-dimensional fermi superfluid: Significance of the confinement-induced effective range of interactions, Phys. Rev. Lett. **122**, 070401 (2019).

[47] X. Y. Yin, H. Hu, and X.-J. Liu, Few-body perspective of a quantum anomaly in two-dimensional fermi gases, Phys. Rev. Lett. **124**, 013401 (2020).

[48] J. H. V. Nguyen, M. C. Tsatsos, D. Luo, A. U. J. Lode, G. D. Telles, V. S. Bagnato, and R. G. Hulet, Parametric excitation of a bose-einstein condensate: From faraday waves to granulation, Phys. Rev. X **9**, 011052 (2019).

[49] D. Linnemann, H. Strobel, W. Muessel, J. Schulz, R. J. Lewis-Swan, K. V. Kheruntsyan, and M. K. Oberthaler, Quantum-enhanced sensing based on time reversal of nonlinear dynamics, Phys. Rev. Lett. **117**, 013001 (2016).